Mechanism of Nucleon Transfer Reactions Induced by 148-MeV N^{14} Ions*

J. BIRNBAUM,† J. C. OVERLEY, AND D. A. BROMLEY
Yale University, New Haven, Connecticut
(Received 28 December 1966)

Neutron and proton transfer reactions have been studied in the $C^{12}+N^{14}$ system using a 148-MeV N^{14} beam and an isotopic identification system capable of resolving isolated residual states. Highly selective population of states having a simple one-nucleon configuration based on the N^{14} ground state has been observed in the $C^{12}(N^{14},O^{15})B^{11}$ and $C^{12}(N^{14},N^{15})C^{11}$ analog reactions. The ratio of cross sections for these reactions is well reproduced on the assumption of charge symmetry. Calculations based on the Boyarkina and on the Kurath wave functions are in agreement with the observed relative population of the ground and first excited states of the $A=11$ mirror pair. None of the transfer angular distributions show diffraction oscillations, contrary to the predictions of the Frahn and Venter model. Both the Dar and the Dodd and Greider models can reproduce experimental results; however, the evidence now available on heavy-ion transfer reactions favors the finite range potential and recoil mechanism of the latter model.

I. INTRODUCTION

THE single-nucleon transfer reaction has been one of the most extensively studied of the nuclear reactions between complex nuclei.[1] However, much of this activity has been confined to energies below the Coulomb barrier, since the experimental and theoretical situations are then somewhat less complex. The present paper presents an experimental investigation of the transfer reactions resulting from the bombardment of a carbon target by 148-MeV nitrogen ions. Information on the elastic and inelastic scattering in this system has been obtained simultaneously.

As the incident energy becomes significantly greater than the Coulomb barrier, the colliding nuclei come into close contact, and the effects of the strong short-range nuclear forces must be considered in any theoretical model of the reaction. Several such models have recently been evolved[2–5] which represent these nuclear effects by strong absorption in the entrance and exit reaction channels. The nucleon (or cluster) transfer is considered as a perturbation of the quasi-elastic interaction of the heavy nuclear cores, and only the encounters in a narrow effective reaction zone at the interaction surface are taken to contribute significantly to the transfer probability.

At the outset of this work specific predictions were available from several of these transfer models concerning the anticipated behavior of the angular distributions at high incident energies. One of the objectives of the present measurements was to test these predictions in detail and, as implied by the predictions, determine the relative importance of the Coulomb and nuclear amplitudes in these reactions. The system selected for study also permits simultaneous examination of neutron and proton transfer reactions involving mirror residual states; it was thus hoped to obtain information on isobaric spin behavior in the tails of the nucleon wave functions, which are preferentially involved in these reactions.

It has been found that the single-nucleon transfer reactions are highly selective in populating residual states, consistent with a simple single-particle transfer mechanism to a predominantly unexcited target core. Measurements on the deuteron transfer reaction leading to states in O^{16} have also been performed and the results are also in qualitative agreement with a simple transfer mechanism.

The transfer reaction angular distributions measured here have not shown the characteristic diffraction oscillation structure predicted by the above-mentioned models; during the course of this work several new theoretical approaches[2–5] have been developed to explain this behavior. The present results will be compared with the predictions of these theories. The inelastic scattering angular distributions do show strong characteristic oscillations, in accord with expectations, and highly selective population of the states of C^{12} which have been excited in other heavy ion inelastic interactions involving the C^{12} nucleus.

In the following sections of this paper, after a brief description of the experimental procedures and data handling, a presentation of the results and a discussion of these results as they bear on both the reaction mechanism and the spectroscopic aspects of the problem are given.

II. EXPERIMENTAL PROCEDURE

All data were taken using the 148-MeV N^{14} beam of the Yale University heavy-ion linear accelerator. The

* This work was supported by the U. S. Atomic Energy Commission.
† Present address: IBM-Watson Research Center, Yorktown Heights, New York.
[1] For reviews of this field see: A. Zucker, Ann. Rev. Nucl. Sci. **10**, 27 (1960); K. R. Greider, Advan. Theoret. Phys. **1**, 245 (1965).
[2] W. E. Frahn and R. H. Venter, Nucl. Phys. **59**, 651 (1964).
[3] A. Dar, Phys. Rev. **139**, B1193 (1965); A. Dar and B. Kozlowsky, Phys. Rev. Letters **15**, 1036 (1965).
[4] L. R. Dodd and K. R. Greider, Phys. Rev. Letters, **14**, 959 (1965).
[5] V. M. Strutinskiĭ, Zh. Experim. i Teor. Fiz. **46**, 2078 (1964) [English transl.: Soviet Phys.—JETP **19**, 1401 (1964)].

beam entered a previously described[6] scattering chamber through two $\frac{1}{8}$-in. collimators and an antiscattering baffle and was incident upon a self-supporting foil of natural carbon. Product nuclei were detected in a ΔE-E particle telescope, also previously described.[6] The ΔE detector is a fast rise-time, high resolution ionization chamber. Under the operating conditions for these experiments, its total equivalent aluminum thickness is 17.4 mg/cm^2, including the $\frac{1}{4}$-mil Mylar windows. A Nuclear Diodes silicon surface barrier detector, with depletion depth 550 μ, was used for the E detector. This detector stopped all nuclei of interest.

Conventional thermionic circuitry provided the initial amplification for the detector signals; further amplification and discrimination were performed by standard transistorized instrumentation.[7] The amplified E and ΔE pulses constituted the direct inputs to a Victoreen 20 000-channel multiparameter pulse-height analyzer.

The ability to identify individual energy states in the product nuclei is crucial to the study of low-yield, high-energy, heavy-ion reactions. This poses a formidable experimental task, reflecting the large number of open reaction channels and the ensuing difficulty in the isolation of a particular nuclide from the plethora of reaction products. The most commonly used technique involves forming the product of the E and ΔE signals. For the nonrelativistic cases under consideration, the Bethe relation[8] for the energy loss of a charged particle traversing matter reduces approximately[6] to

$$(dE/dx) = -(KMZ^2/E), \qquad (1)$$

where M and Z are the mass and charge of the particle, respectively, and K is a physical constant. Since MZ^2 is a unique quantity for all known nuclear species (provided Z is the atomic number of the isotope, which is well approximated[9] in the reactions under consideration) the E-ΔE product may serve as a particle identification pulse, and is usually used to gate a multichannel analyzer so that only the desired energy spectrum is stored.

In the present work, the multiparameter analyzer was gated by an internal 1-μsec coincidence between the ΔE and E signals. In this way, the approximately hyperbolic loci (Eq. 1) corresponding to individual isotopes are stored directly in the magnetic core memory of the analyzer, without the need for pulse multiplication. Any portion of the spectrum may be expanded for more detailed examination through the use of variable-gain window amplifiers, which are an integral part of the analyzer input circuitry. Contour, isometric, and planar section displays are available at all times. The memory contents are conveniently and rapidly written on computer compatible magnetic tape.

A computer program has been developed[10] for the IBM 7040/7094 computer which, after locating the trace corresponding to any given isotope, transforms the two-dimensional $\Delta E \times E$ array into a conventional energy spectrum. Locations of the individual isotopic loci are specified by several (x,y) addresses selected from the map display. A least-squares fit of these points with a modified form of the Bethe equation yields parameters which serve to define the locus of each isotope.

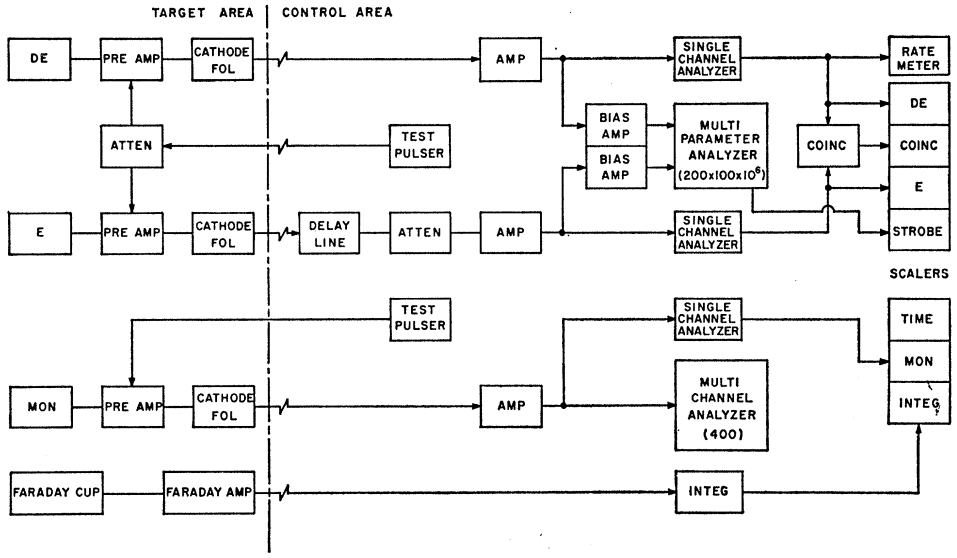

FIG. 1. Block diagram of the electronic system.

[6] M. W. Sachs, C. Chasman, and D. A. Bromley, Phys. Rev. **139**, B92 (1965) and references contained therein.
[7] C. E. L. Gingell, IEEE Trans. Nucl. Sci. **N510**, 32 (1963).
[8] H. A. Bethe, Ann. Physik, **5**, 325 (1930).
[9] L. C. Northcliffe, Phys. Rev. **120**, 1744 (1960) and J. Birnbaum (private communication).
[10] J. Birnbaum, Ph.D. thesis, Yale University, 1966 (unpublished).

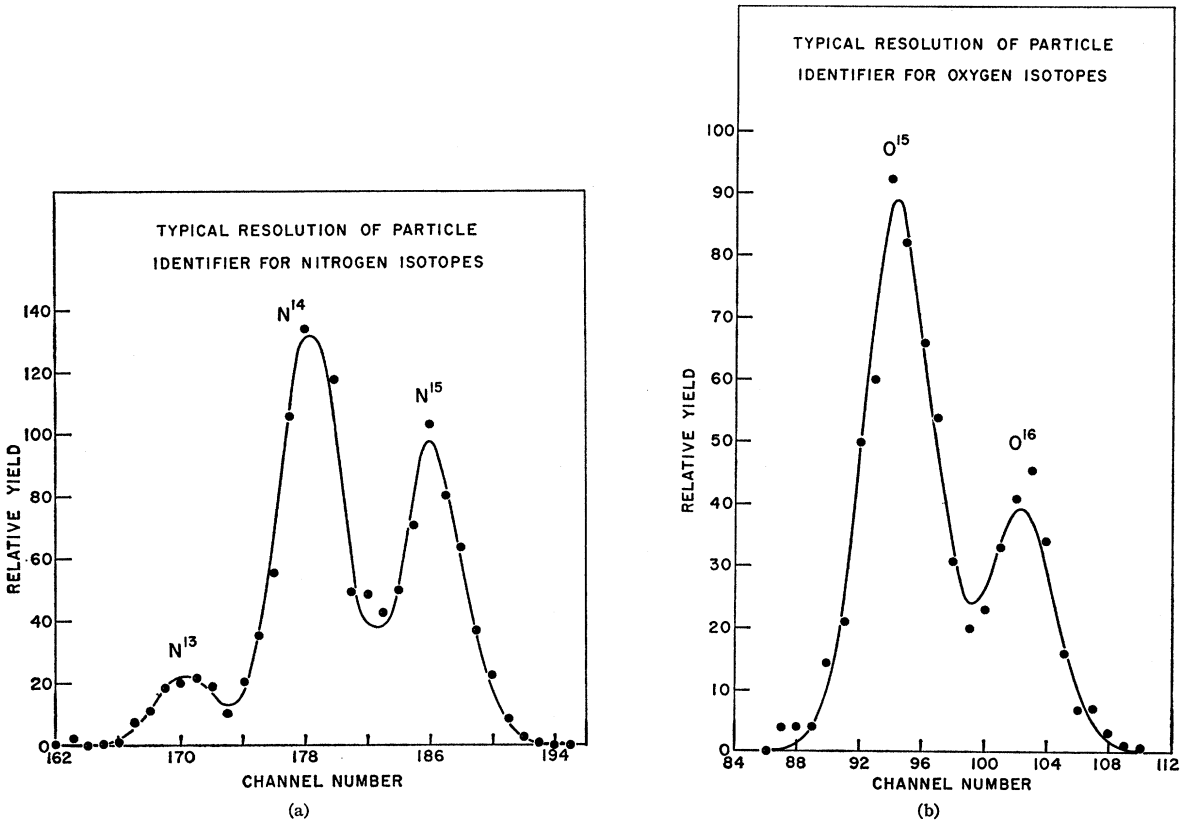

FIG. 2. Resolution of the particle identifier for the isotopes of (a) nitrogen and (b) oxygen, respectively. The curves shown are the computer fits to the data.

The measured response function of the ΔE detector is then fitted to the family of isotopic loci corresponding to an element, using nonlinear least-squares techniques. The above-mentioned corrected energy spectra are synthesized from these results. Using similar techniques, the E detector response function is then used to extract yields and excitation energies from the resultant spectra. Energy losses in the windows and the transmission counter, and physical quantities of interest such as center of mass angles, momentum transfers, etc. are calculated in the process.

Apart from the ease and flexibility of this mode of operation, it provides the ability to collect data simultaneously on several nuclear reactions resulting from the same combination of target and projectile; data so acquired are expected to be of high internal consistency since they are free from normalization and calibration errors. Figure 1 is a block diagram of the instrumentation used for the present experiment. The isotopic resolution achieved is illustrated in Fig. 2. Figure 3 is a contour representation of the nitrogen and oxygen reaction products.

(a) (b) (c)

FIG. 3. (a) Contour map of the MPA memory contents, showing from right to left, the loci corresponding to the isotopes of oxygen, nitrogen, and part of carbon. The ordinate is E and the abscissa ΔE. Note the effect of the biased amplifiers. Thresholds were set as follows, where z represents the number of counts in a given channel: $z<100$=blank; $100\leq z<1000$=low intensity; $1000\leq z\leq 10000$ =high intensity; $10000\leq z$=blank. Note the analogous structure in N^{15} and O^{15}, and the high peaks corresponding to elastic and inelastic scattering. This figure was generated on an IBM 7040/7094 computer. (b) Same as (a), but lower thresholds changed to highlight the structure: $z<200$=blank. The peak in the upper right-hand corner is due to the calibration pulser. (c) "Isometric" plot of the data shown in (a) and (b).

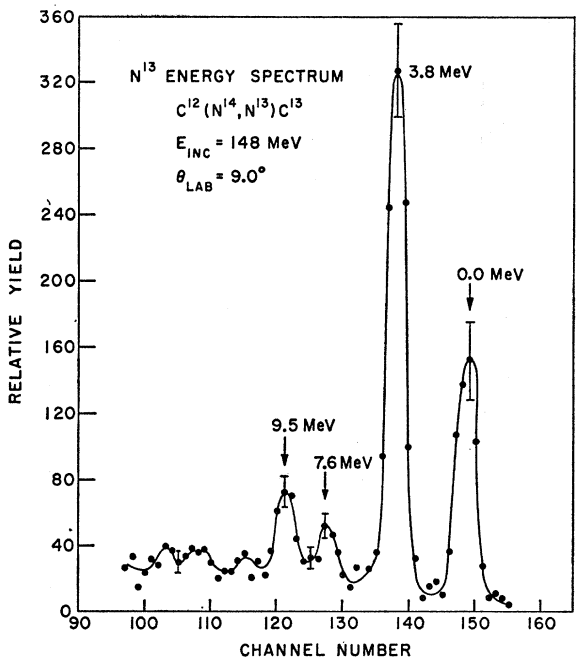

FIG. 4. N^{13} energy spectrum, $C^{12}(N^{14},N^{13})C^{13}$. The errors shown reflect statistical errors as well as the quality of the isotopic resolution in a given channel. The solid lines simply connect the experimental points.

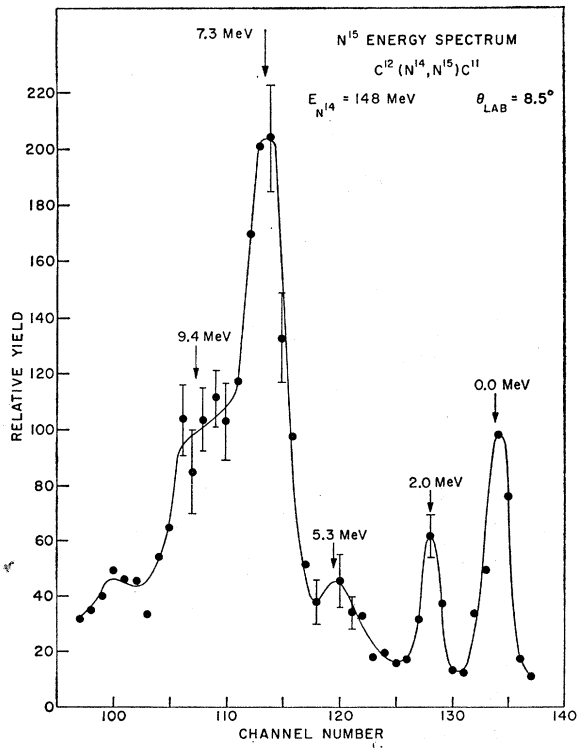

FIG. 5. N^{15} energy spectrum, $C^{12}(N^{14},N^{15})C^{11}$. Error bars and solid curve have same significance as in Fig. 4.

The carbon targets used for this work were prepared by standard vacuum evaporation and flotation techniques. Cross sections are normalized to a target thickness of 210 ± 30 $\mu g/cm^2$, determined by weighing and by α-particle range measurements. C^{13} is present in these targets in its natural isotopic abundance of 1.1%; its contribution to the reactions under discussion was shown to be negligible by comparing results obtained with gaseous targets of natural methane with those from a 59% C^{13}-enriched methane target. The transmitted beam was collected in a shielded Faraday cup, and integrated beam charge was measured by an Elcor

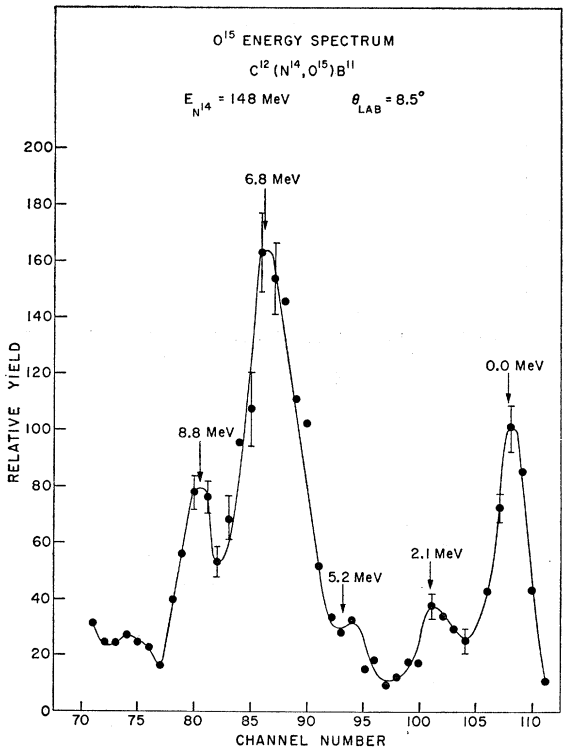

FIG. 6. O^{15} energy spectrum, $C^{12}(N^{14},O^{15})B^{11}$. Error bars and solid curve have same significance as in Fig. 4.

model A309 A current integrator. Secondary electron effects were suppressed through the use of a permanent magnet trap.

The detector telescope subtended a solid angle of 4.9×10^{-5} sr at the target and corresponded to an angular acceptance of 1°10′.

The energy resolution of the system for 148-MeV N^{14} ions elastically scattered from a thin gold calibration target was 0.9%, with major contributions from the energy spread of the beam and the uncertainty of the energy loss in the ionization chamber. The resolution of the latter instrument for the same case is 3.6%.

Calibration of the analyzer energy scale was accomplished by elastically scattering the beam from targets

of varying mass and taking these energies as known. The range energy curves of Northcliffe[11] were used to correct for the energy losses in the ionization chamber. The absolute accuracy of this procedure is dependent upon knowledge of the beam energy, considered determined to within 0.6% by a previously calibrated magnetic momentum analysis system. However, the energy relative to a given peak in an energy spectrum is known to within 300 keV, and, in practice, the absolute energy calibration is also within 300 keV.

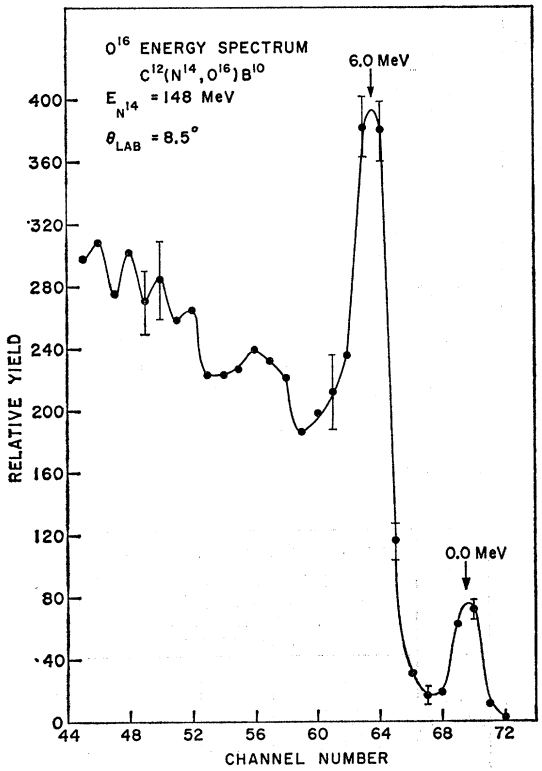

FIG. 7. O^{16} energy spectrum, $C^{12}(N^{14},O^{16})B^{10}$. Error bars and solid curve have same significance as in Fig. 4.

III. EXPERIMENTAL RESULTS

Energy spectra for the reactions $C^{12}(N^{14},N^{13})C^{13}$, $C^{12}(N^{14},N^{15})C^{11}$, $C^{12}(N^{14},O^{15})B^{11}$, $C^{12}(N^{14},O^{16})B^{10}$, and for N^{14}-C^{12} elastic and inelastic scattering are shown in Figs. 4–8. Since heavy-particle stripping is expected to be negligible[12] at the forward angles investigated in this work, the first four reactions are taken to represent neutron stripping, and neutron, proton, and deuteron pickup, respectively. The identifiable peaks are labeled with excitation energies in the observed product nucleus; the values are averages obtained from least-squares fits of measured peak shapes to these spectra. The variation of the fitted values of these excitation energies was within the stated relative energy resolution of 0.3 MeV in all cases. The error bars shown on the figures reflect both the counting statistics and the effects of background due to adjacent isotopes. They were calculated under the assumption that the variances of the parameters associated with the isotopic fits are normally distributed.[10]

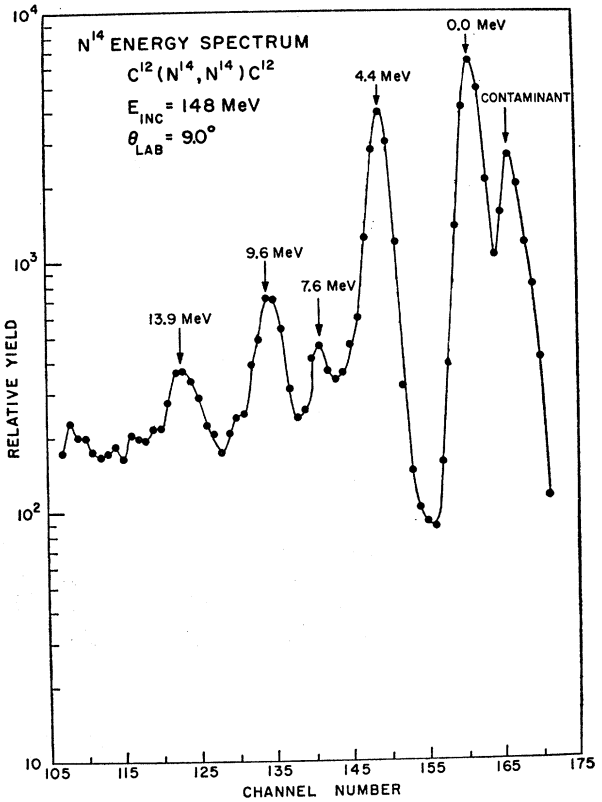

FIG. 8. N^{14} energy spectrum, $C^{12}(N^{14},N^{14})C^{12}$. The significance of the error bars and the solid line is as in Fig. 4.

Angular distributions of the resolvable levels for the various reactions are presented in Figs. 9–13 in the form of center-of-mass differential cross section versus center-of-mass scattering angle.

Tables I and II presents the absolute total cross sections for the transfer reactions. It has been assumed that the angular dependence of the differential cross section may be represented by a pure exponential:

$$(d\sigma/d\Omega)=\sigma_0 e^{-\alpha\theta},$$

with

$$\sigma_{\text{total}}=2\pi\int_0^{\pi}\left(\frac{d\sigma}{d\Omega}\right)\sin\theta d\theta.$$

The cross sections are to be interpreted as being those

[11] L. C. Northcliffe (private communication and to be published).

[12] M. K. Banerjee, in *Nuclear Spectroscopy*, edited by F. Ajzenberg-Selove (Academic Press Inc., New York, 1960), *Part B*, p. 727.

arising strictly from the forward-angle transfer process previously indicated for each reaction. That is, any contributions from large-angle heavy-particle stripping are ignored.[12] The principal contribution to the reaction cross section should come from the angular interval studied, as any sharp rise at forward angles is nullified by the small value of $\sin\theta$, and large-angle contributions are negligible due to the exponential factor.

The absolute accuracy of the cross sections, within these assumptions, is $\pm 25\%$.

IV. DISCUSSION AND COMPARISON WITH THEORY

A. Selective Population in the Single-Nucleon-Transfer Reactions

The most striking features of the energy spectra of Figs. (4)-(8) are the relatively few levels strongly excited, and the fact that the ground and low-lying levels are considerably less populated than levels of higher excitation. These effects have been previously observed in nucleon transfer reactions induced by both light[13] and heavy[6] projectiles.

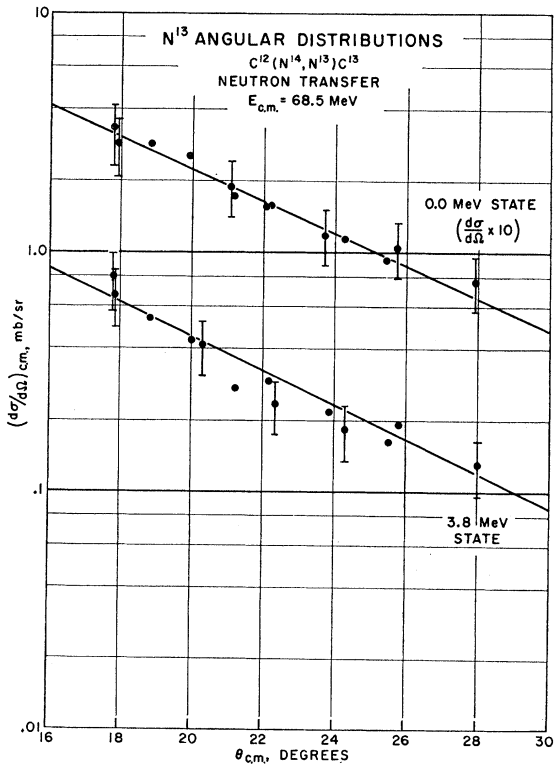

FIG. 9. N^{13} angular distributions, $C^{12}(N^{14},N^{13})C^{13}$. In Figs. 9–12, the lines shown are drawn through the experimental points, and are taken to have equal slope for convenience. Absolute errors are indicated.

[13] For example, B. G. Harvey, J. Cerny, R. H. Pehl, and E. Rivet, Nucl. Phys. **39**, 160 (1962) and references therein.

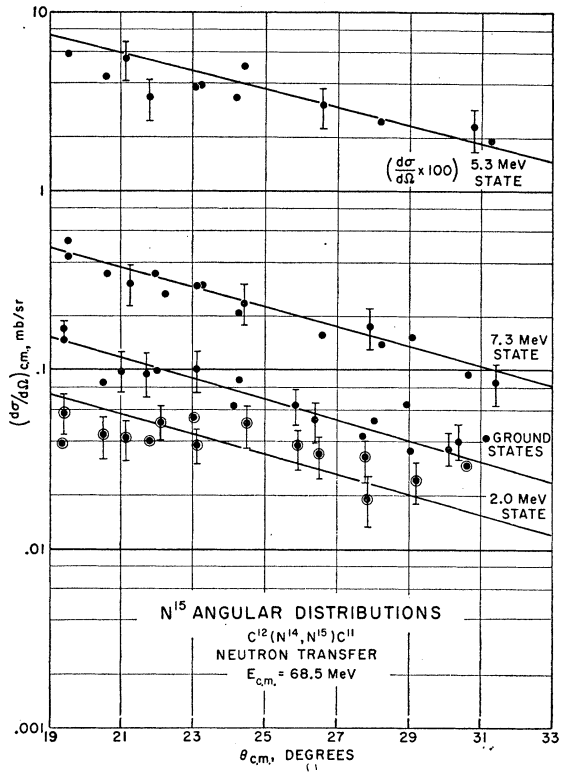

FIG. 10. N^{15} angular distributions, $C^{12}(N^{14},N^{15})C^{11}$.

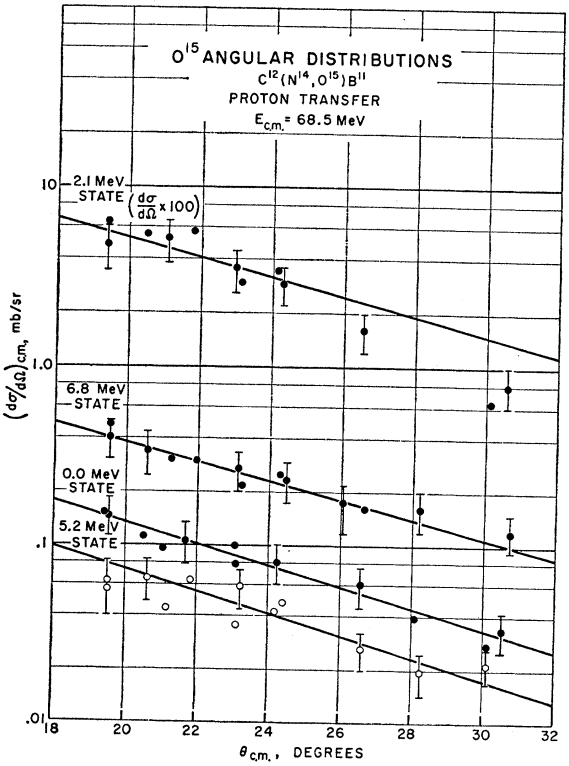

FIG. 11. O^{15} Angular distributions, $C^{12}(N^{14},O^{15})B^{11}$.

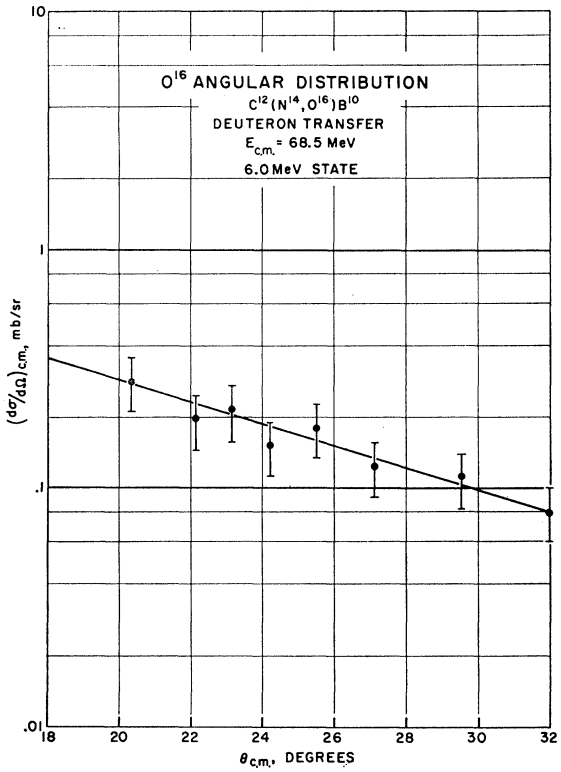

FIG. 12. O^{16} angular distribution, $C^{12}(N^{14},O^{16})B^{10}$.

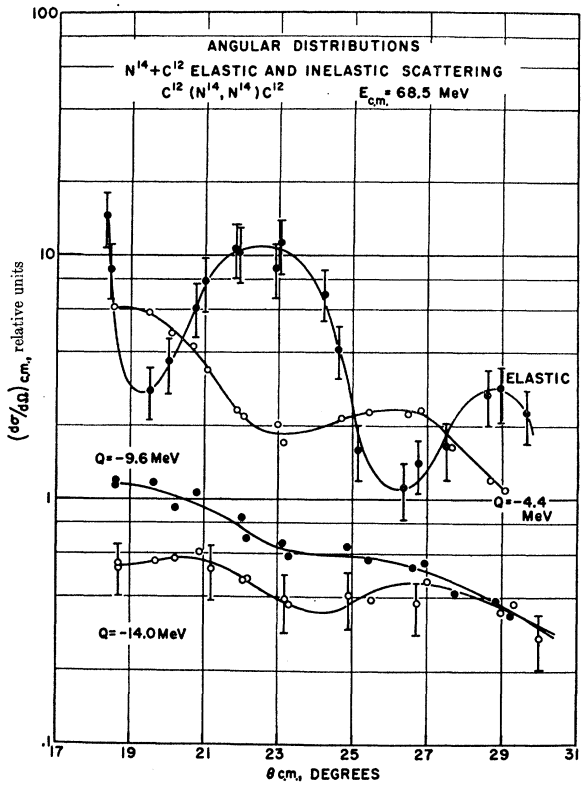

FIG. 13. N^{14} angular distributions, $N^{14}+C^{12}$ elastic and inelastic scattering. The curves are drawn through the experimental points; absolute errors are indicated.

It will be shown in the following discussion of the individual reactions that the levels selectively populated are consistent with a simple model for the reaction. A necessary condition for the excitation of a level appears to be that the level have a dominant single particle configuration of core plus transferred nucleon. Since no states with the character of an excited core

TABLE I. Total reaction cross sections for the $C^{12}(N^{14},N^{15})C^{11}$ and $C^{12}(N^{14},O^{15})B^{11}$ mirror reactions, assuming only neutron and proton transfer, respectively.[a]

Observed nucleus		N^{15}	O^{15}	N^{15}	O^{15}	N^{15}	O^{15}	N^{15}	O^{15}
Final-state excitation		Ground states	Ground states	2.0 MeV in C^{11}	2.1 MeV in B^{11}	5.3 MeV in N^{15}	5.2 MeV in O^{15}	7.3 MeV in N^{15}	6.8 MeV in O^{15}
Functional parameters	α	7.19	6.91	7.19	6.91	7.19	6.91	7.19	6.91
	σ_0, mb	1.52	1.22	0.779	0.544	0.87	0.63	5.18	4.10
σ_{Total}, mb		0.181	0.158	0.092	0.071	0.103	0.082	0.616	0.530
$(\sigma_{\text{Total}}/\sigma_{\text{Geometric}})$		1.3×10^{-4}	1.1×10^{-4}	6.4×10^{-5}	4.9×10^{-5}	7.1×10^{-5}	5.7×10^{-5}	4.3×10^{-4}	3.7×10^{-4}

[a] $E_{c.m.}=68.5$ MeV, $\sigma_{\text{Geometric}}=\pi r_0^2(A_1^{1/3}+A_2^{1/3})$, $r_0=1.45$ F, $\sigma_G=1450$ mb, $d\sigma/d\Omega=\sigma_0 e^{-\alpha\theta}$, and α for c.m. angles in radians.

TABLE II. Total reaction cross sections for the $C^{12}(N^{14},N^{13})C^{13}$ and $C^{12}(N^{14},O^{16})B^{10}$ reaction, assuming only neutron and deuteron transfer, respectively.[a]

Reaction	$C^{12}(N^{14},N^{13})C^{13}$		$C^{12}(N^{14},O^{16})B^{10}$	
Transferred particle	Neutron	Neutron	Deuteron	Deuteron
Final-state excitation, MeV	Ground states	3.8 in N^{13}	Ground states	6.0 in O^{16}
Functional parameters α	9.07	9.07	···	5.90
σ_0, mb	5.2	10.7	···	2.16
σ_{Total}, mb	0.39	0.81	<0.05	0.24
$\sigma_{\text{Geometric}}$, mb	1450	1450	1450	1450
$(\sigma_{\text{Total}}/\sigma_{\text{Geometric}})$	2.69×10^{-4}	5.57×10^{-4}	$<3.5\times10^{-5}$	1.66×10^{-4}

[a] $E_{c.m.}=68.5$ MeV, $\sigma_{\text{Geometric}}=\pi r_0^2(A_1^{1/3}+A_2^{1/3})$, $r_0=1.45$ F, $d\sigma/d\Omega=\sigma_0 e^{-\alpha\theta}$, and α for c.m. angles in radians.

coupled to the transferred nucleon were observed to be strongly populated, this suggests that the transfer proceeds predominantly by means of a simple one-stage process.

The factors determining the relative strengths of the transfers to levels satisfying the above conditions are not obvious. The appropriate single-particle nature of a state appears to be a necessary but not sufficient condition for its strong population. Pehl[14] has suggested, on intuitive grounds, that those levels for which the angular momentum transferred in the reaction most nearly matches the angular momentum of the shell model orbit into which the nucleon is transferred, will be most strongly populated. This argument has recently been given a sounder basis by the work of Dodd and Greider.[4] These authors, by using a finite-range potential, and retaining terms involving the recoil momentum of a residual nucleus in the phase of the wave functions describing the scattering, have shown that the population of states of low angular momentum is inhibited at high incident-ion energies.

1. $C^{12}(N^{14},N^{13})C^{13}$

Figure 4 presents the energy spectrum at 9.0° for this neutron stripping reaction. Two strong peaks, at excitation energies of 0.0 and 3.8 MeV are observed, with weaker excitations at 7.6 and 9.5 MeV. In each case the indicated excitations represent averages over all angles considered. All excitations, other than that at 0.0 MeV, must correspond to excited levels of C^{13}, since only the ground state of N^{13} is stable against particle emission, with the result that N^{13} nuclei in excited states do not have adequate lifetime to enable them to reach the detectors.

If this reaction is viewed as $C^{12}+(N^{13}+n)\rightarrow N^{13}+(C^{12}+n)$, then, on the basis of the simple reaction model discussed above, the states populated are expected to have dominant parentage (C^{12}(g.s.)$+n$). Evidence for at least four states of this character has been found previously[15]: 0.0 MeV ($J^\pi=\frac{1}{2}^-$), 3.09 MeV ($J^\pi=\frac{1}{2}^+$), 3.85 MeV ($J^\pi=\frac{5}{2}^+$), and 7.68 MeV ($J^\pi=\frac{3}{2}^+$).

The state observed at 0.0 MeV is identified as that corresponding to both product nuclei in their ground states. The half-width of the peak at 3.8 MeV is consistent, on the basis of the known purity of the ground-state peak, with the excitation of a single level in C^{13}. The 3.85-MeV level is the most probable assignment for this level. Tombrello and Phillips[16] have calculated that this level has a parentage of 0.986 for the (C^{12}(g.s.)$+n$) configuration, with the neutron in a relative $d_{5/2}$ orbit. The 3.68-MeV level in C^{13}, which apparently is not strongly excited in this reaction, is predicted[15] to have strong parentage based on C^{12*} (4.43 MeV, $J^\pi=2^+$) and a $p_{3/2}$ neutron.

The observed excitation at 7.6 MeV may be tentatively identified as the $\frac{3}{2}^+$ state at 7.68 MeV, with strong parentage[15] for (C^{12}(g.s.)$+d_{3/2}$ neutron). The much smaller population of this state relative to the 3.8-MeV level may reflect a more complex configuration for the upper state.

The most probable assignment for the level at an indicated excitation of 9.5 MeV is the 9.51-Mev ($J^\pi=\frac{7}{2}^-$) state in C^{13}. This level exhibits a resonance for the scattering of 4.95-MeV neutrons and it is of interest to note that McGruer *et al.*[17] in a study of the $C^{12}(d,p)C^{13}$ reaction at $E_d=14.8$ MeV, found that this state was relatively weakly excited, with an angular distribution consistent with $l=3$ neutron transfer, suggesting a configuration of (C^{12}(g.s.)$+f_{7/2}$ neutron). Strong ground-state parentage for the state is also suggested by weak population of the state through the $C^{12}(n,n'\gamma)C^{12}$ inelastic scattering reaction proceeding to the 4.43-MeV level of C^{12}.[18]

2. $C^{12}(N^{14},N^{15})C^{11}$

The 9° energy spectrum is shown in Fig. 5. In this reaction it is no longer possible to ascribe the observed excitation definitely to one product nucleus on physical grounds. The distinguishable excitations are 0.0, 2.0, and 5.3 MeV. There is a broad intense group centered at 7.3 MeV, with a wide shoulder on the high-excitation side.

As before, on the basis of a direct transfer, the states most strongly populated are expected to be those whose dominant configuration is N^{14}(g.s.)+neutron. The excitation corresponding to both product nuclei in their ground states is consistent with the N^{14}(g.s.)$+p_{1/2}$ neutron configuration of the N^{15} ground state. The small peak on the low-energy side of the ground state can only be the 1.99-MeV first excited state of C^{11}, since the first excited level of N^{15} is more than 3 MeV higher. In a simplified distorted-wave Born approximation treatment, which neglects the effects of spin-flip, and assumes that the effective transfer function is relatively insensitive to details of nuclear structure and remains essentially constant for reactions leading to adjacent states in a given nucleus,[19] the cross section ratio for these states reduces to a ratio of spectroscopic factors for the C^{11} states involved. This calculation has been performed, using the intermediate-coupling shell-model wave functions of Boyarkina,[20] yielding a cross-section ratio of 2.7, in good agreement with the experimentally

[14] R. H. Pehl, Ph.D. thesis, University of California, Lawrence Radiation Laboratory Report No. UCRL-10993 (unpublished).
[15] G. C. Phillips and T. A. Tombrello, Nucl. Phys. **19**, 555 (1960), and references therein.
[16] T. A. Tombrello and G. C. Phillips, Nucl. Phys. **20**, 648 (1960).
[17] J. N. McGruer, E. K. Warburton, and R. S. Bender, Phys. Rev. **100**, 235 (1955).
[18] W. Hall and T. Bonner, Nucl. Phys. **14**, 295 (1959).
[19] J. E. Poth, Ph.D. thesis, Yale University, 1966 (unpublished); Phys. Rev. (to be published).
[20] A. N. Boyarkina, Izv. Akad. Nauk USSR **28**, 337 (1964).

observed ratio of about 2. Kurath[21] has calculated a relative strength of 3.8 for transitions to these levels.

There is no evidence for any significant excitation of the 4.26- and 4.75-MeV levels of C^{11}. The weak excitation at 5.3 MeV may be identified as corresponding to the 5.270-MeV and 5.299-MeV levels of N^{15}, since no levels of C^{11} occur at this energy, within the system resolution. The energy resolution is not sufficient to distinguish between these levels. Their weak population is consistent with the intermediate shell model calculations of Halbert and French[22] who find that these states are based primarily on an excited N^{14} core [N^{14}(2.31 MeV)0^+, $T=1$]. Only states with dominant $T=0$ parentage should be significantly populated in this reaction, assuming isospin conservation. This assignment is further borne out by the reaction

$$C^{15} \underset{\beta-}{\longrightarrow} N^{15}(5.3\ \text{MeV}),$$

which is observed[23] to be a favored transition, indicating the $T=1$ nature of the N^{14} core for this level.

No excitation of the 6.33-MeV level was observed; this is in accord with the single-hole character (O^{16}(g.s.) $+p_{3/2}$ hole) long associated[24] with this state. However, Bock *et al.*,[25] in a study of the $B^{11}(O^{16},N^{15})C^{12}$ reaction with 30-MeV O^{16} ions, saw this state populated only half as strongly as the ground state in a reaction which should be equally preferential in selecting single hole configurations. The relatively weak excitation in the O^{16}-induced reaction and the total nonobservance in the present measurements may be explained on the basis of the recent work of Lopes *et al.*[26] Through a systematic study of the mixing ratios of the $\frac{3}{2}^-$ to $\frac{1}{2}^-$, 6.15- and 6.33-MeV-to-ground γ transitions in O^{15} and N^{15}, respectively, it has been demonstrated that both states are principally collective in character, with strong parentage based on the 6.92-MeV ($J^\pi=2^+$) state in O^{16}. This state has recently been demonstrated to form the band head of a strongly deformed rotational band in O^{16}. Thus the $B^{11}(O^{16},N^{15})C^{12}$ reaction to this state proceeds through the smaller component of the wave function based on the O^{16} ground state.

Computer fits to the group at 7.3 MeV indicate that the major excitation probably corresponds to the excitation of two levels, with two or more additional levels contributing to the broad shoulder. Definite identification is not within the scope of the present measurements, but some conjectures as to the most probable excitations are possible. The states in N^{15} at 7.16 MeV ($J^\pi=\frac{5}{2}^+$), 7.31 MeV ($J^\pi=\frac{3}{2}^+$) and 7.57 MeV ($J^\pi=\frac{7}{2}^+$) are all based, in large degree, on the N^{14} ground-state core, according to shell model calculations,[22] which also find large neutron reduced widths for all three levels.

Warburton *et al.*[27] have advanced convincing arguments for identification of the 6.79-MeV state in O^{15} as the mirror partner of this 7.31-MeV state and, as will be noted later, in the mirror reaction the 6.79-MeV state can be more clearly resolved as that receiving the dominant population in the proton transfer. Furthermore, Marion *et al.*[28] have observed a strong threshold for this state in the $N^{14}(d,n)O^{15}$ reaction, confirming its dominant single particle parentage. It also appears strongly in the $N^{14}(p,\gamma)O^{15}$ reaction.[29] All these data would lead to identification of the 7.31-MeV state in N^{15} as the dominant excitation in the neutron transfer. There is one piece of contradictory evidence, however, in that the C^{15} beta decay is reported to feed the 7.31-MeV state in N^{15} with a logft value between 4 and 5,[30] suggesting a significant parentage component of the state based on the $T=1$ first excited state of N^{14}, which is inaccessible to the neutron transfer reaction.

Similarly, the favored β-decay of C^{15} to the 8.31-MeV N^{15} level,[23] suggests that this level will not be strongly excited in the present reaction, despite its predicted dominant configuration[21] of an $s_{1/2}$ neutron coupled to the N^{14} g.s. core, and its large neutron reduced width. A large component of the 8.57-MeV level is probably[31] (N^{14}(g.s.)$+d$ nucleon) and so population of this level is indicated.

Little can be deduced concerning levels above this except that excitation of the 9.05-MeV level of N^{15} is not expected since the β-decay of C^{15} to this level is super-allowed[30] indicating that the $T=0$ component of the wave function must be small. The 9.22-MeV state appears the most probable candidate in this region, since the 9.16-MeV level is based on a (N^{14}(g.s.)+hole) configuration. Because the states of N^{15} and of C^{11} are unbound against neutron and α-particle emission at excitations of 10.208 and 7.544 MeV, respectively, it would not be anticipated that such excitations significantly in excess of 10.208 MeV would be observed. It is clear from the spectra that N^{15} nuclei are observed at energies which correspond to this forbidden region. These may arise from two sources. The first is mutual excitation wherein the transfer process leaves both nuclei in excited states. The excitation at 9.3 MeV, for example, very probably corresponds to simultaneous population of the strong 7.3-MeV state in N^{15} and the 2.0-MeV state in C^{11}. Both the energies and the rela-

[21] D. Kurath (private communication to D. A. Bromley).
[22] E. C. Halbert and J. B. French, Phys. Rev. **105**, 1563 (1957).
[23] D. E. Alburger, A. Gallmann, and D. H. Wilkinson, Phys. Rev. **116**, 939 (1959).
[24] I. Talmi and I. Unna, Ann. Rev. Nucl. Sci. **10**, 353 (1960).
[25] R. Bock, H. H. Duhn, M. Grosse-Schulte, and R. Rüdel, Phys. Letters **18**, 45 (1965).
[26] J. S. Lopes, O. Hausser, H. J. Rose, A. R. Poletti, and M. F. Thomas, Nucl. Phys. **76**, 223 (1966).
[27] E. K. Warburton, J. W. Olness, and D. E. Alburger, Phys. Rev. **140**, B1202 (1965).
[28] J. B. Marion, R. M. Brugger, and T. W. Bonner, Phys. Rev. **100**, 46 (1955).
[29] D. Povh and D. F. Hebbard, Phys. Rev. **115**, 608 (1959).
[30] D. E. Alburger (private communication to D. A. Bromley).
[31] D. Pelte, B. Povh, and W. Scholz, Nucl. Phys. **78**, 241 (1966).

tive intensities are consistent with such an explanation. The second source follows population of N^{16} and O^{16} at excitations in excess of their neutron and proton binding energies, respectively, with the consequence that prior to reaching the detector telescope these states decay into N^{15}+nucleon leaving a low-energy N^{15} to be detected.

3. $C^{12}(N^{14},O^{15})B^{11}$

The 8.5° energy spectrum is presented in Fig. 6. In the limit of the charge symmetry of nuclear forces, the energy spectra of the mirror products N^{15} and O^{15} should be identical, with the arguments presented above for N^{15} carrying over to O^{15} without change. Comparison of Fig. 5 and Fig. 6 with the analog levels indicated in the level diagram of Fig. 14 indicates the accord with this expectation. The spectra appear essentially identical from the ground level to the large excitations at 7.3 MeV and 6.8 MeV in N^{15} and O^{15}, respectively. The 0.0-, 2.1-, 6.2-, and 6.8-MeV peaks may be identified with the ground state, 2.14-MeV level in B^{11}, the 5.188- and 5.240-MeV levels, and the excitations at 6.79, 6.85, and 7.17 MeV, respectively. The 6.16-MeV state is not observed, for the same reason that the 6.33-MeV state is absent in the N^{15} spectrum.

The fact that the major peak at 6.8 MeV is sharper than its analog at 7.3 MeV in N^{15} reflects the fact that no O^{15} levels above 7.291 MeV will be detected because of the neutron emission threshold at this energy. The equivalent threshold in N^{15} does not occur until 10.208 MeV, explaining the relative breadth of the low energy shoulder.

The peak at ~8.8 MeV may well correspond to formation of the 6.8-MeV levels of O^{15} with the residual

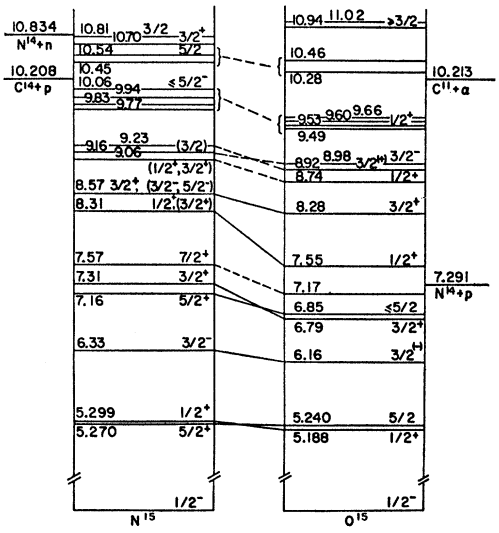

FIG. 14. Energy level diagram of N^{15} and O^{15}, with analog levels indicated. Correspondences thought certain are indicated by solid lines; those less certain or speculative are shown by the dashed lines. (From Ref. 27).

B^{11} left in its 2.14-MeV first excited level, as observed for the ground state and 2.1-MeV peaks. The ratio of peak heights is very similar in the two cases, lending support to this interpretation.

4. $C^{12}(N^{14},O^{16})B^{10}$

The energy spectrum at 8.5° is shown in Fig. 7. Although this reaction has been referred to as "deuteron" transfer above, this is not to be interpreted as necessarily representing the transfer of a physical deuteron, but simply a neutron-proton pair. However, the similarity of the selection mechanism for strong population and previous similar results for both light and heavy projectiles[6,12] indicates that the two nucleons are transferred as a cluster. Only two resolvable excitations, at 0.0 and 6.0 MeV are observed. The former clearly corresponds to ground-state population; the latter represents excitation of one or both of the levels at 6.05 MeV ($J^\pi=0^+$) and 6.13 MeV ($J^\pi=3^-$). Kelson[32] has calculated that the 6.13-MeV level has dominant configuration $d_{5/2}(p_{1/2})^{-1}$ and is largely a single-particle state; the 6.05-MeV state, on the other hand, exhibits 98% "collective" behavior (two or more particle excitation). A distinction between these possibilities requires a more detailed treatment of the two particle transfer mechanism than is presently available.

B. Relative Cross Sections in the $C^{12}(N^{14},N^{15})C^{11}$ and $C^{12}(N^{14},O^{15})B^{11}$ Mirror Reactions

The mirror reactions

$$C^{12}(N^{14},N^{15})C^{11} \quad \text{and} \quad C^{12}(N^{14},O^{15})B^{11}$$

should, in the limit of the charge symmetry of nuclear forces, manifest essentially identical characteristics. Apart from small differences in the kinematic factors involved, negligible in the context of the present discussion, the absolute cross sections for reactions leading to analog states in the mirror nuclei should be identical if the transition matrix elements are charge-independent.

If the neutron and proton transfer reactions are charge independent, then the cross section is proportional to

$$(d\sigma/d\Omega)\sim(k_f/k_i)(T_aT_c;\ T_{za}T_{zb}-T_{za}|T_bT_{zb})^2 \times(T_AT_c;\ T_{zA}T_{zB}-T_{zA}|T_BT_{zB})^2|T_{fi}|^2. \quad (2)$$

T_{fi} is the transition amplitude for the reaction symbolically represented by $A(a,b)B$ where $a=(b+c)$, $B=(c+A)$ and c is the transferred nucleon. T_i is the isotopic spin of particle i, T_{zi} is its projection, and T_{fi} is assumed to contain only charge-independent terms. The terms in brackets are the familiar Clebsch-Gordan vector addition coefficients.

With these assumptions, T_{fi} is identical for the population of analog states in these mirror reactions, and

[32] I. Kelson, Phys. Letters **16**, 143 (1965).

the ratio of reaction cross sections for the neutron and proton transfers is simply given by the ratio of the appropriate vector coupling coefficients and phase space factors.

Robson[33] has proposed that the nuclear interior is generally a region of relatively pure isospin, and that the most significant mixing of isospins, if any, will occur in an exterior region. The present reactions should be particularly sensitive to such an effect, since the interactions are localized at the nuclear surface. The reactions differ from those discussed by Robson in that he treats resonances in the continuum whereas the present work is concerned with discrete bound levels.

Numerous experimental investigations of cross section ratios for reactions leading to isobaric analog states have been reported using light projectiles[34]; that is, in situations where the nuclear interior might be expected to play a significant role. In all cases in which appropriate kinematic conditions were fulfilled, the observed cross section ratios reported have been reproduced by the simple isospin Clebsch-Gordan factor. It was therefore of interest to test these predictions in the case of heavy-ion reactions to search for any effect indicating enhanced isospin mixing in the external regions preferentially involved.

For the N^{15} and O^{15} mirror reactions, the ratio of the cross sections, following the above assumptions, may be expressed as

$$\frac{(d\sigma/d\Omega_n)}{(d\sigma/d\Omega_p)}=(k_n/k_p)\frac{(0\tfrac{1}{2};\,0\tfrac{1}{2}|\tfrac{1}{2}\tfrac{1}{2})^2}{(0\tfrac{1}{2};\,0-\tfrac{1}{2}|\tfrac{1}{2}-\tfrac{1}{2})^2}\times\frac{(0\tfrac{1}{2};\,0-\tfrac{1}{2}|\tfrac{1}{2}-\tfrac{1}{2})^2}{(0\tfrac{1}{2};\,0\tfrac{1}{2}|\tfrac{1}{2}\tfrac{1}{2})^2}\cdots \quad (3)$$
$$=(k_n/k_p)\sim 1\,,$$

where the subscripts n and p refer to the neutron and proton transfer reactions, respectively, and k is the exit channel wave number. The ratio of k_n to k_p is unity to within $\frac{1}{2}\%$ because the Q values of the reactions are almost identical.

In order to compare the N^{15}-O^{15} experimental yields, the sum of all counts below corresponding excitations in the energy spectra of the two nuclei was computed using the level relations shown in Fig. 14. This is a more reliable procedure than comparing the relative cross sections of individual analog states, for the latter procedure would then involve any errors introduced in the unfolding of each spectrum. The summation procedure is justified by the fact that *all* levels in one nucleus have an analog in the spectrum of the mirror product. Because of the large difference in the particle emission thresholds of N^{15} and O^{15}, as noted above, and the necessity for summing only corresponding levels in the two nuclei, the sum was restricted to the ground- and first-excited-state peaks. This method of summation, although limited, should be quite reliable. After appropriate background subtraction the mean ratio of the N^{15} to the O^{15} cross sections in measurements at 12 angles in the range 19 to 30 deg, center of mass, was found to be 1.02 ± 0.10. Clearly, more accurate measurements are needed; however, within the present experimental uncertainty, there is no evidence which would suggest any enhanced isospin mixing in the nuclear surface regions.

C. Transfer Reaction Angular Distributions

The angular distributions for the transfer reactions studied are presented in Figs. 9–12. The nonoscillatory nature of these distributions is in disagreement with the predictions of the reaction models available at the outset of these measurements.[2] The models predicted strong oscillations, resulting from modulation of the smooth Coulombic angular distribution by the nuclear reaction amplitudes.

During the course of this work, and, in part, in consequence of the smooth angular distributions reported herein, two new reaction models have been evolved[3,4] which appear capable of reproducing the experimental findings. In these models the mechanisms proposed as responsible for the removal of the diffraction oscillations are quite different. These models will be considered briefly and their predictions compared with the experimental results.

The diffraction model of Frahn and Venter[2] for single-nucleon transfer reactions between complex nuclei is based upon a strong absorption formalism developed by these authors[35] for the elastic scattering of complex nuclei. Within this framework, the transfer reaction is regarded as a quasi-elastic process, with the strong absorption condition introduced by means of a scattering function in l space which is approximately a step function in the region corresponding to the interaction surface. That is, the collision partners are viewed as moving along classical Coulomb trajectories, little affected by the transfer; since the scattering function essentially vanishes in the nuclear interior, the only significant probability for transfer occurs in a narrow effective reaction zone at the nuclear surface.

The result obtained is

$$(d\sigma/d\theta)=\tau^2T'/k^2(F_-)^2\times[1+(F_+/F_-)^2+2(F_+/F_-)\sin(2T'\theta)], \quad (4)$$

where $F_\pm$ is given by

$$F_\pm=F[\Delta'(\theta\pm\theta_{c'})]=\frac{\pi\Delta'(\theta\pm\theta_{c'})}{\sinh\pi\Delta'(\theta\pm\theta_{c'})}; \quad (5)$$

[33] D. Robson, Phys. Rev. **137**, B535 (1965).

[34] D. A. Bromley, E. Almqvist, H. E. Gove, A. E. Litherland, E. B. Paul, and A. J. Ferguson, Phys. Rev. **105**, 957 (1957); J. Cerny and R. H. Pehl, Phys. Rev. Letters **12**, 619 (1964).

[35] R. H. Venter and W. E. Frahn, Ann. Phys. (N. Y.) **27**, 401 (1964) and references therein.

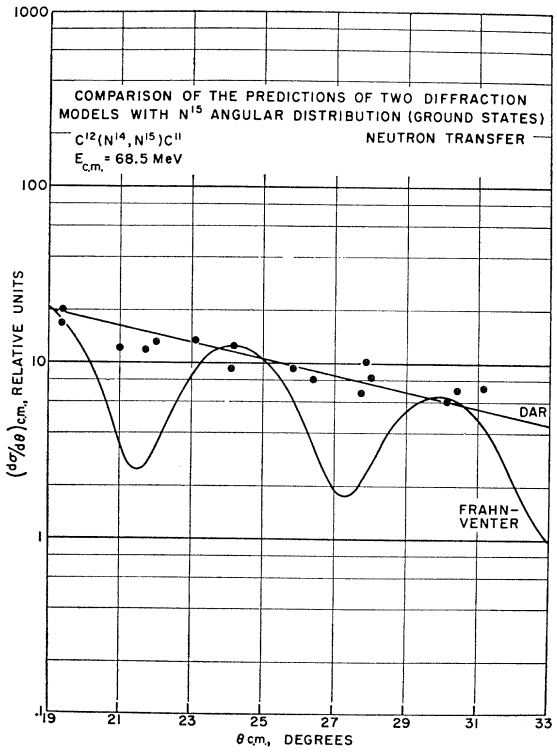

FIG. 15. Comparison of the predictions of the Frahn-Venter and of the Dar diffraction models with the experimental angular distribution for the $C^{12}(N^{14},N^{15})C^{11}$ (g.s.) reaction. The curves have been arbitrarily normalized to the data. The interference term has been neglected in the Dar calculation. The surface diffuseness parameter, d, was taken to be 0.39 F and 0.2 F, in the Frahn-Venter and Dar calculations, respectively.

where θ_c' is the classical scattering angle corresponding to a grazing collision, τ is a measure of the strength of the transfer, and $T'=L+\frac{1}{2}$, where L is the angular momentum corresponding to some defined interaction radius. Δ' is a parameter which is related to the surface diffuseness in l space, k is the relative wave number, η is the Coulomb parameter, and R is a suitably defined interaction radius.

Equation (4) consists of a smoothly varying part and an oscillatory term proportional to $\sin(2T'\theta)$. The oscillations will be damped when Coulomb effects are dominant, that is, when $(4\pi\eta d/R)\gg 1$. The condition is satisfied for heavy ion reactions at low energies and at medium-to-high energies when large Z targets are used (i.e., when η is large). Prior to the initiation of the present work, no measurement had been carried out in the appropriate energy range, and with sufficient angular detail to detect the predicted oscillations. The Coulomb damping condition is not satisfied for the reactions presently under consideration because of the small (~ 2) value of η. Frahn and Venter suggest[2] that the observation of the predicted oscillations in the non-Coulomb damped case would constitute a crucial test of their model. Such oscillations would also provide useful information concerning the relative contributions of Coulomb and nuclear amplitudes to the cross section, since the oscillations are of nuclear origin.

Figure 15 compares the experimental angular distribution of the $C^{12}(N^{14},N^{15})C^{11}$(g.s.) reaction with the prediction of Eq. (4) for this case. The calculated oscillations are well outside the experimental uncertainties. Similar results were obtained for all transfer reactions studied, leading to the conclusion that a damping mechanism other than that attributable to Coulomb effects is involved.

Dar and his collaborators[3] have recently provided an alternate formulation for heavy-ion transfer reactions which under certain conditions can predict smooth angular distributions. Dar's finite range diffraction model is a natural extension of the work of Frahn and Venter, but there are several significant differences. Principal among these is that Dar's is a three-body, rather than an "equivalent" two-body, theory, with provision for an interaction potential between the transferred cluster and the heavy cores. Coulomb effects and nuclear structure effects (e.g., specific angular-momentum transfers) are included explicitly in the formalism. The physical picture is that of Coulomb waves diffracting around a strongly absorbing nucleus. Finite effects are treated directly as a consequence of the fact that the only wave functions that appear in the overlap integrals for the transition matrix elements are the Coulomb waves and the tails of the bound-state wave functions, since the distorted waves are assumed to vanish in the strongly absorbing nuclear interior and in the classical shadow regions. Outside of these areas, the Coulomb waves are assumed undistorted, and the overlap integrals are evaluated in Coulomb-wave Born approximation. A type of WKB approximation is employed to replace the Coulomb waves by their less cumbersome classical counterparts. The dominant interaction is taken to be between the transferred cluster and the heavy aggregate to which it is not bound. The method of partial waves is used, with a diffuse surface assumed for the nucleus (this is equivalent to a smooth cutoff of the low-l partial waves). The resultant angular distribution prediction is given by

$$(d\sigma/d\theta)\sim\frac{1}{\cosh^2[\pi\delta(\theta-\theta_c')]-\cos^2[\pi\delta(\Delta'/2)]}+\frac{1}{\cosh^2[\pi\delta(\theta-\theta_c')]-\cos^2[\pi\delta(\Delta'/2)]}$$
$$+\frac{(-1)^l\{\cosh(2\pi\delta\theta_c')-\cos(\pi\delta\Delta)\cosh(2\pi\delta\theta)\cos[(2L_\theta+1)\theta-\pi/2]-\sin(\pi\delta\Delta)\sinh(2\pi\delta\theta)\sin[(2L_\theta+1)\theta-\pi/2]\}}{\{\cosh^2[\pi\delta(\theta-\theta_c')]-\cos^2[\pi\delta(\Delta'/2)]\}\{\cosh^2[\pi\delta(\theta+\theta_c')]-\cos^2[\pi\delta(\Delta'/2)]\}},\quad(6)$$

where θ is the center-of-mass scattering angle, $\theta_{c'}$ is the scattering angle for Coulombic trajectories corresponding to an apsidal distance equal to the interaction radius, $(\Delta'/2)$ is the ratio of the wave number for the binding of cluster to core to the wave number for the relative motion, both quantities being averaged over the entrance and exit channels. The diffuseness in l space is represented by δ, which is equivalent to the symbol Δ used by Frahn and Venter. L_0 is the angular momentum corresponding to a grazing collision, and l denotes the angular momentum transferred in the reaction.

The first two terms are smoothly varying, while the last term is oscillatory. Under the conditions required for Coulomb damping, as outlined for the Frahn-Venter model, the interference term becomes negligible, and remaining terms provide excellent fits to the smoothly varying angular distributions observed experimentally for energies below the Coulomb barrier, or for reactions with large values of η. For the case of negligible Coulomb effects (small η) and high energy, Dar also neglects the interference term, but for a different reason.

If the transferred cluster is in definite subshells $l_i j_i$, $l_f j_f$ in the projectile and final nucleus, respectively, then the following selection rules are obtained[3]: (i) $l+l_i+l_f$ even; (ii) $l_i-l_f \leq l \leq l_i+l_f$; (iii) $j_i-j_f<l<j_i+j_f$. In consequence of (i), the phase of the interference term is proportional to $(-1)^{l_i+l_f}$. For the case of negligible Coulomb damping, Dar concludes:

(a) The transfer of a cluster from a definite subshell $l_i j_i$ to a definite subshell $l_f j_f$ should always exhibit an oscillatory structure. Transitions with the same parity (or l_i+l_f) are in phase, those of different parity are out of phase.

(b) The sum over l implicit in the derivation of Eq. (6) can produce a damping of the oscillations if both odd and even values of l are involved. This situation can result only from a configuration mixing for the transferred particle.

(c) Mixing of l values with different parity may also be the result of a particle transfer accompanied by a core excitation.

If condition (b) and/or (c) is assumed to hold for the present reactions, and only the first two terms of Eq. (6) are used on the grounds that the sum over contributing l values will lead to effective cancellation of the interference term, good agreement with the present results is obtained, as illustrated in Figs. 15 and 16. Although Dar's treatment contains specific factors for the absolute magnitude of the cross section, their evaluation awaits the development of suitable bound-state wave functions for the heavy nuclei involved. Therefore, the curves have been arbitrarily normalized and displaced for clarity. The value of the surface diffuseness used for all fits was 0.2 F, which is in agreement with values obtained from other heavy ion reactions.[3] Although somewhat better fits could have been obtained by varying this parameter, the slight modifications did not seem justified in view of the magnitude of the experimental errors.

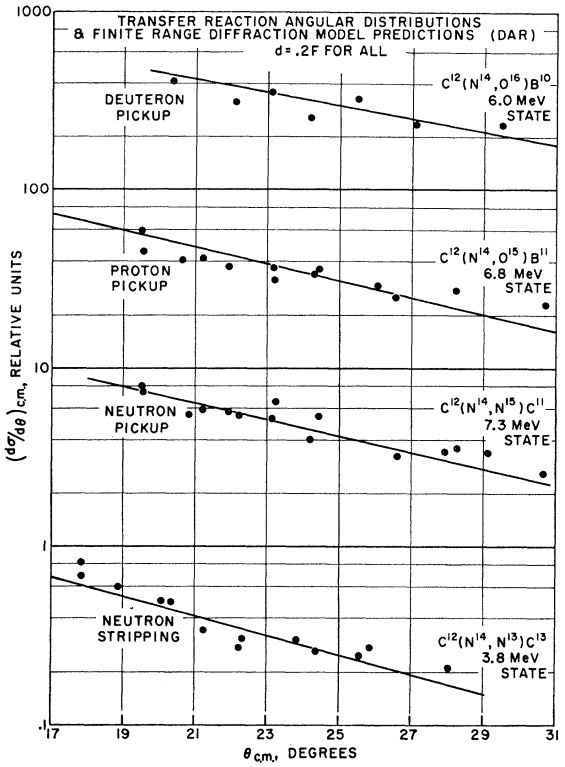

FIG. 16. Comparison of the Dar model predictions with the experimental angular distributions for various transfer reactions. The curves have been arbitrarily normalized and displaced for clarity.

Despite the satisfactory fits attained using the Dar theory, the degree of configuration mixing which these fits would imply is surprising, particularly when it is noted that all measured angular distributions to all final states studied show the same smooth behavior.

An alternate explanation for the smoothness of the experimental angular distributions which avoids this difficulty has recently been suggested by Dodd and Greider.[4] These authors show that if finite potential range *and* recoil terms (that is, terms proportional to $1/A$, where A is the ratio of the mass of a heavy core to the mass of the transferred cluster bound to that core) are properly accounted for, then a smooth angular distribution results. The effect is independent of the reaction model chosen and is a reflection of the three-body nature of the transfer process.

The damping effect is brought about by retaining the recoil terms in the phase of the transition matrix elements which results in an extra phase factor that multiplies the interaction operator. For transfers induced by light projectiles (e.g., deuteron stripping), this recoil term has little effect because the interaction

operator has short range. However, in cases of nucleon transfer between two heavy nuclei, the recoil phase factor can damp the diffraction oscillations completely because the interaction operator has longer range.

Dodd and Greider have evaluated a simple case in distorted-wave Born approximation without spin effects, assuming harmonic oscillator wave functions for the bound states, a Gaussian finite-range interaction potential, and an $l=0$ to $l=L$ transition.[4]

With the assumption of a sharp cutoff for l, the analytical solution for $L>1$ and angular-momentum transfer, q, large is

$$\left(\frac{d\sigma_2}{d\Omega}\right) \xrightarrow[q\gg 1/a]{} \frac{1}{q^3}\exp\left(-\frac{p^2a^2}{6}\right), \tag{7}$$

where a is the range of the bound-state wave function, and p is given by $p=(k_i/A_i+k_f/A_f)$, with k_i, k_f the relative wave numbers and A_i, A_f the mass ratios of core to cluster, in the entrance and exit channels, respectively. Dodd and Greider propose that the monotonic angular dependence pertains to generalized $l=L'\rightarrow l=L$ transitions, since the expression for the cross section was found to be independent of angular momentum. A given experiment will, in general, include mixtures of several values of transferred angular momentum, each of which should yield the same q dependence.

A more recent calculation, employing more realistic assumptions,[36] indicates that the q dependence of the angular distribution may be better represented by q^{-4} than by q^{-3}. Several representative distributions are presented as a function of q in Fig. (17), with the Dodd-Greider predictions indicated (the slowly varying exponential factor has been neglected). The points have been arbitrarily normalized. As indicated, good agreement is obtained with the experimental data.

Durand[37] has recently provided a further approach to this problem based upon the observation that multiparticle problems can be reformulated by replacing composite systems by "elementary" particles with vanishing wave function renormalization constant. In this formulation, the recoil effects noted above appear as simple kinematic consequences of the model. In addition, the dependence of the cross section on q is in agreement with the result of Dodd and Greider, as is the prediction that the population of states of low angular momenta will be inhibited at high energies.

It is interesting to note that the independence of the transfer cross section upon all details of the reaction as found by Dodd and Greider and by Durand is quite the obverse of the result of Dar, who bases his explanation of the smooth angular distributions on the specific structure of the nuclei involved, and ignores the effects of momentum recoil in his derivation.

[36] L. R. Dodd and K. R. Greider (private communication to J. Birnbaum.)
[37] L. Durand (unpublished).

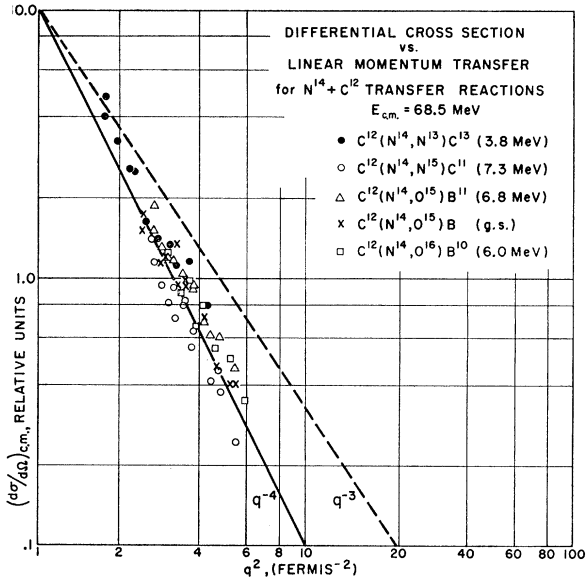

FIG. 17. Representative transfer reaction differential cross sections as a function of linear momentum transfer q. The predictions of Dodd and Greider are shown. The data have been arbitrarily normalized.

A definitive experiment, which was not possible with the facilities available for the present work, would involve the variation of the incident energy in a transfer reaction study over a broad range. If recoil effects are indeed responsible for the damping of the oscillatory structure in the angular distributions then this structure should reappear at lower energies, i.e., lower recoil. On the other hand, if angular-momentum effects dominate, as suggested by Dar, the characteristics of the angular distributions should not change with energy.

The present measurements demonstrate that the Frahn-Venter treatment of the transfer reactions is inadequate at high energies where Coulomb effects are small. Determination of the relative importance of Coulomb and nuclear amplitudes, as implicit in the model, is therefore precluded.

D. Elastic and Inelastic Scattering in the N^{14}-C^{12} System

The energy spectrum of N^{14} at 8.5° is shown in Fig. 8; the angular distributions for resolvable levels are presented in Fig. 13. While both the elastic and inelastic scattering of complex nuclei constitute problems of considerable current interest, it is not within the scope of the present work to present a detailed quantitative analysis of these reactions. However, two features of the results are immediately apparent:

(i) A highly selective inelastic scattering mechanism is involved;

(ii) the angular distributions for both the elastic and inelastic scattering are highly oscillatory in nature,

in qualitative agreement with the results of experiments on similar systems.[38–40]

The second point is especially important in the context of this paper: since all data were obtained simultaneously, the presence of oscillations in the elastic and inelastic scattering distributions lends credence to the smooth angular distributions observed for the transfer reactions.

The first point is in accord with the previously reported[41] preferential excitation of collective levels in the inelastic scattering of heavy ions. The principal excitations observed at 4.4, 9.6, and 13.9 MeV may be identified as the 4.43-, 9.63-, and 14.0-±0.5-MeV states in C^{12}. These states have been previously observed[39–42] in the inelastic scattering of $O^{16}+C^{12}$, and of $C^{12}+C^{12}$.

No evidence for the population of the 2.313-MeV level ($J^\pi=0^+$, $T=1$) was found; formation of this state would constitute a violation of isobaric spin conservation. The state is also of single-particle character and so its excitation is not expected. The small peak on the low energy side of the 4.4-MeV excitation corresponds to an average excitation of 7.6 MeV, although the statistics are quite poor. The excitation may be the 7.66-MeV state ($J^\pi=0^+$) in C^{12}, previously observed to be weakly populated in inelastic scattering from a carbon target.[42]

The phenomenon of mutual excitation, observed in both the C^{12}-C^{12} and O^{16}-C^{12} systems,[40–42] was not observed in this reaction. This is a reflection of the fact that no individual states of N^{14} are excited strongly enough to contribute significantly to the process; this this would seem to indicate that the populated states in carbon are much more collective in character than any states in N^{14}.

The angular distributions of the inelastically excited states are in agreement with the phase rule of Blair.[43] The angular distribution of the 9.63-MeV ($J^\pi=3^-$) level, expected to be in phase with the elastic scattering is quite structureless, in agreement with previous measurements.[41] The shape of the angular distributions for the elastic scattering is in reasonable agreement with an earlier measurement,[38] although the ranges of angles studied do not overlap appreciably.

As discussed by Garvey,[41] the relative steepness of the envelope of the angular distributions is directly related to the number of phonons producing the excitation. This quantity is approximated by finding the ratio of successive maxima for a given excitation. The results are compared in Table III with the averaged values obtained for C^{12}-C^{12} scattering,[41] O^{16}-C^{12} scattering,[42] and values obtained by Garvey[41] from a universal curve for (α,α') scattering. Good agreement with the previous measurements is found.

TABLE III. Average steepness of inelastic-scattering angular distributions.

Reaction Q, MeV	No. phonons	(N^{14},C^{12})	(C^{12},C^{12})	(O^{16},C^{12})	(α,α')
0	0	3.8	5.4	4.5	4.1
−4.43	1	2.6	2.8	2.6	2.4
−14.0	2	1.3	1.5	...	...

V. SUMMARY

All the single-nucleon transfer reactions studied herein have been observed to exhibit highly selective population of individual states, with a characteristic inhibition of the low-lying levels relative to states of intermediate excitation (~6–9 MeV). Levels of a single-particle nature with dominant configuration of core plus transferred nucleon are preferentially excited, with the angular momentum of the transferred nucleon a controlling factor in the population of a given level. States involving low angular-momentum transfer are inhibited with optimum conditions arising when the angular momentum carried by the transferred nucleon matches the angular momentum of the shell-model orbit into which the nucleon is transferred (2 or 3 units in the cases studied). A theoretical basis for this phenomenon has recently been proposed by Dodd and Greider.[4]

The angular distributions for the transfer reactions were all found to be smoothly varying and approximately exponential, in disagreement with the predictions of the Frahn-Venter diffraction model[2] which predicts a highly oscillatory distribution. The extension of this model to the high energy, low η case appears unjustified. Recently, two different mechanisms have been proposed to account for this absence of diffractive behavior. Dar's explanation involves the mixing of out-of-phase contributions to the cross section as a result of configuration mixing or core excitation[3]; Dodd and Greider[4] show that the observed exponential dependence is predicted if a finite range potential is used in the derivation of the transition amplitude and if recoil terms are retained in the phase of the transfer matrix elements. The former explanation is strongly dependent upon the structure of the nuclei involved, whereas the latter is almost entirely independent of it. The ubiquity of the smooth angular distribution in presently available high-energy heavy-ion studies appears to favor the latter explanation.

[38] A. M. Smith and F. E. Steigert, Phys. Rev. **125**, 988 (1962); E. Newman, P. G. Roll, and F. E. Steigert, *ibid.* **122**, 1842 (1961).
[39] G. T. Garvey and J. C. Hiebert in *Proceedings of the Third International Conference on Reactions Between Complex Nuclei, Asilomar, 1963*, edited by A. Ghiorso, R. M. Diamond, and H. E. Conzett (University of California Press, Berkeley, 1963) p. 36.
[40] G. T. Garvey, A. M. Smith, J. C. Hiebert, and F. E. Steigert, Phys. Rev. Letters **8**, 25 (1962); G. T. Garvey, A. M. Smith, and J. C. Hiebert, Phys. Rev. **130**, 2397 (1963).
[41] G. T. Garvey, Ph.D. thesis, Yale University, 1962, and references therein (unpublished).
[42] J. C. Hiebert, Ph.D. thesis, Yale University, 1963, and references therein (unpublished).
[43] J. S. Blair, Phys. Rev. **115**, 928 (1959).

The mirror reactions involving proton and neutron transfers are in accord with predictions based on the charge symmetric nature of nuclear forces. The measured absolute cross sections for the formation of analog states are equal, within the accuracy of the present experiment, consistent with isospin remaining a good quantum number in the nuclear surface regions. More precise measurements on such systems will be required to determine small isospin mixing effects.

The elastic and inelastic scattering differential cross sections display characteristic oscillations. The inelastic scattering selectively populates states of collective character in C^{12}, in agreement with previous measurements on similar heavy-ion reactions.

ACKNOWLEDGMENTS

We are indebted to Dr. J. Poth for his assistance in developing the techniques and apparatus described herein, and for sharing the taking of data; to Dr. K. Nagatani for his aid in data-taking. We thank Dr. M. W. Sachs for many discussions and assistance in the early stages of the computer programming. We are grateful to Dr. K. R. Greider, Dr. L. Dodd, Dr. A. Dar, and Dr. W. E. Frahn for invaluable discussions and communication of the results of their work prior to publication. We acknowledge the assistance of C. E. L. Gingell with the electronic instrumentation and thank the staffs of the Yale heavy-ion linear accelerator and Yale Computer Center.

PHYSICAL REVIEW VOLUME 157, NUMBER 4 20 MAY 1967

De-Excitation of Highly Excited Nuclei*

J. Robb Grover
Chemistry Department, Brookhaven National Laboratory, Upton, New York

AND

Jacob Gilat†
Chemistry Department, State University of New York at Stony Brook, Stony Brook, New York and Chemistry Department, Brookhaven National Laboratory, Upton, New York

(Received 29 July 1966)

We describe a scheme of calculations useful for computer evaluation of the de-excitation of nuclei having large excitation energies and angular momenta. The scheme is based on the statistical model. Cascade emission of γ rays is taken into account. In particular, we include consideration of both dipole and quadrupole γ-ray emission, and of the crucial role played by the lowest excited state at every angular momentum in the nuclei involved. We are thus, for example, in a position to study phenomena connected with particle emission following γ-ray emission. As input in a sample calculation ($Ce^{140}+O^{16}$ at 90 MeV, lab) we use information obtained from experimental data and from the optical and shell models, but independent of the data with which comparisons are made. We find generally reasonable agreement, and no serious disagreements, with a variety of experimental data, with no parameter adjustment. The predicted energy spectra of emitted α particles and γ rays show important features not demonstrated in previous, less complete calculations. The γ spectrum displays a low average energy of less than 1.0 MeV. The number of photons emitted by quadrupole radiation is typically of the same order of magnitude as the number emitted by dipole radiation. Other results are also described.

INTRODUCTION

To interpret measurements on many nuclear reactions, it is useful to know accurately the relevant behavior predicted by the nuclear-evaporation model. Until recently, however, predictions exact and complete enough to represent adequately the consequences of this model were restricted to the small ranges of excitation energy and angular momentum within which they could be calculated. These ranges can now be greatly extended, because the use of very fast computers having large memories makes it feasible to cope with the voluminous bookkeeping such calculations entail.

Perhaps more important than the newly developed capacity to analyze old data is the prospect of learning something new about nuclei. When the calculations are carried completely through, previously unsuspected consequences of the theory are revealed, and these in turn suggest new experiments. A recent, familiar example of this synergy is the recognition[1] that the analysis of a compound-nucleus excitation function can provide an estimate of the energy of the lowest excited state at each angular momentum in the product nucleus,

* Research performed in part under the auspices of the U. S. Atomic Energy Commission.

† Present address: Israel Atomic Energy Commission, Soreq Nuclear Research Center, Yavne, Israel.

[1] J. R. Grover, Phys. Rev. **127**, 2142 (1962).

(a) (b) (c)

FIG. 3. (a) Contour map of the MPA memory contents, showing from right to left, the loci corresponding to the isotopes of oxygen, nitrogen, and part of carbon. The ordinate is E and the abscissa ΔE. Note the effect of the biased amplifiers. Thresholds were set as follows, where z represents the number of counts in a given channel: $z<100$ = blank; $100\leq z<1000$ = low intensity; $1000\leq z\leq 10000$ = high intensity; $10000\leq z$ = blank. Note the analogous structure in N^{15} and O^{15}, and the high peaks corresponding to elastic and inelastic scattering. This figure was generated on an IBM 7040/7094 computer. (b) Same as (a), but lower thresholds changed to highlight the structure: $z<200$ = blank. The peak in the upper right-hand corner is due to the calibration pulser. (c) "Isometric" plot of the data shown in (a) and (b).